

Multi-scale surface texture to improve blue response of nanoporous black silicon solar cells

Fatima Toor,^{a)} Howard M. Branz, Matthew R. Page, Kim M. Jones, and Hao-Chih Yuan
National Renewable Energy Laboratory, 1617 Cole Boulevard, Golden, Colorado 80401, USA

(Received 29 April 2011; accepted 11 August 2011; published online 6 September 2011)

We characterize the optical and carrier-collection physics of multi-scale textured p-type black Si solar cells with conversion efficiency of 17.1%. The multi-scale texture is achieved by combining density-graded nanoporous layer made by metal-assisted etching with micron-scale pyramid texture. We found that (1) reducing the thickness of nanostructured Si layer improves the short-wavelength spectral response and (2) multi-scale texture permits thinning of the nanostructured layer while maintaining low surface reflection. We have reduced the nanostructured layer thickness by 60% while retaining a solar-spectrum-averaged black Si reflectance of less than 2%. Spectral response at 450 nm has improved from 57% to 71%. © 2011 American Institute of Physics. [doi:10.1063/1.3636105]

Photons reflected from a photovoltaic cell surface are not absorbed, nor converted to electricity. Normally, antireflection (AR) in single-crystal (100) silicon solar cells is achieved by coating quarter-wavelength-thick silicon nitride (SiN_x) atop pyramidal surface structures that are 5 to 15 μm tall. The AR coating thickness is designed to provide near-perfect destructive Bragg interference for normal-incidence light at a wavelength near the peak of the usable solar spectrum, but there is inevitably reflection at other wavelengths. The pyramid texture is easily formed on (100) Si by an alkali-etch,^{1,2} based, for example, on potassium hydroxide.¹ In multi-crystalline Si solar cells, an acid etch provides a different micron-scale texture beneath the interference layer.³ These micron-scale textures enhance photon absorption mainly by a geometric optics effect, giving some of the reflected light a second chance to enter Si. Interference-based AR coatings, such as SiN_x , add significant cost per unit cell area to photovoltaic (PV) manufacturing since they are deposited in costly vacuum deposition tools and can require pyrophoric production gases such as silane. However, even when deposited on pyramids, the coatings exhibit narrow-band and poor angular acceptance of incident photons. Therefore, many research groups explore the use of a nanostructured black Si surface to obtain broadband and wide angle-of-view AR in Si.⁴⁻⁹

We previously demonstrated a 16.8%-efficient solar cell with a nanoporous surface AR formed by a one-step Au-nanoparticle-assisted liquid etch on planar Si.⁵ Nanostructured black Si is antireflective due to a graded index of refraction that precludes Fresnel reflection at a sharp surface interface with air or a low-index encapsulation medium; the surface reflection decreases exponentially with the density-graded depth, d , if the nanostructure's lateral scale is much smaller than the wavelength of the light in Si.⁶ In addition, the black Si provides broader band and wider angle-of-view AR than quarter-wavelength interference coatings.^{10,11} However, absorption of short-wavelength photons in the high-recombination nanoporous black Si surface causes poor blue

response that limits the short-circuit current density (J_{sc}). This near-surface recombination also reduces the cell open-circuit voltage (V_{oc}).⁵

In this work, we incorporate multi-scale texture into black Si solar cells by combining pyramid texture and nanostructuring¹²⁻¹⁴ and investigate the optical and electrical performance. We find that the pyramids allow us to reduce the nanoporous Si depth, d , while maintaining excellent black Si AR properties. We fabricated an independently confirmed 17.1%-efficient multi-scale textured Si solar cell, with the increased efficiency due primarily to higher J_{sc} . Adding micron-scale features to combine geometric and black Si, optical effects allows us to reduce the nanostructured surface area and, therefore, the number of photocarriers lost to recombination at and near the surface. It is likely that all nanostructured solar cells, whether of black Si, Si nanowires,¹⁵ nanostructured polymer-fullerene composite,¹⁶ or some other material, will need to employ similar light-management techniques to minimize surface area.

We fabricate multi-scale textured solar cells on 300- μm -thick p-type float-zone (FZ) Si (100) wafers with resistivity of 2.7 $\Omega\text{-cm}$. We first pyramid-texture the Si wafer in 600-ml 2.5% KOH in de-ionized (DI) water and 200-ml isopropanol alcohol solution with N_2 bubbling¹⁷ for 25 min at 80°C. We then remove any potassium impurities in 1:1:5 HCl:H₂O₂:H₂O mixture at 80°C for 10 min. Next, a 1 to 3 min one-step black etch is performed on the front side of the pyramid textured substrate (backside protected with paraffin) by immersing the substrate in 0.4-mM HAuCl₄ solution in a sonication bath and adding an equal volume of 1:5:2 HF:H₂O₂:H₂O mixture to form Au nanoparticles that catalyze the metal-assisted etch.⁶ Residual Au impurities are then removed from the nanoporous surface by immersing the substrate in I₂/KI solution. We described our black Si solar cell structure and the remainder of the fabrication procedure in Ref. 5. Aside from the lack of any SiN_x AR coating, the solar cell fabrication is close to the industry standard for p-type Si, with diffused n^+ POCl_3 emitter, thermal oxide surface passivation, evaporated Ag top contacts, and p^+ Al back-surface-field. We also process nanoporous black Si on

^{a)} Author to whom all correspondence should be addressed. Electronic mail: Fatima.Toor@nrel.gov.

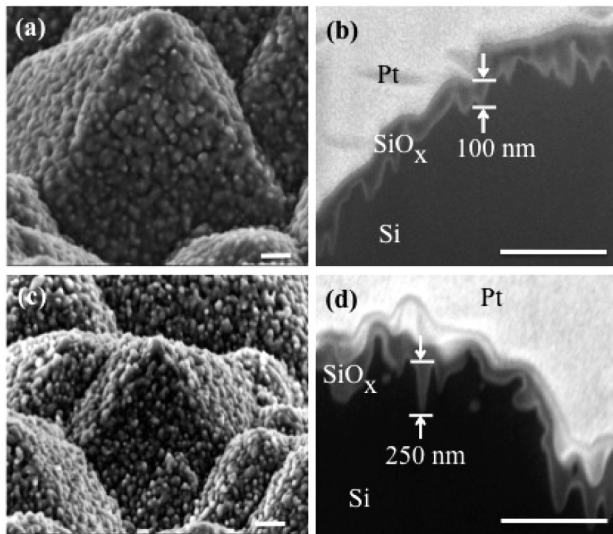


FIG. 1. Tilted top-view (left) and cross-sectional (right) SEM images of multi-scale textured Si solar cells after (a) and (b) 1.5 min and (c) and (d) 3 min metal-assisted nanostructured black-etch followed by solar cell processing. The separation of the two arrow tips in each cross-sectional image indicates typical pore depths for the processed cells. All white scale bars are 500 nm.

planar substrates without the pyramid texture step as a control.

Fig. 1 presents tilted and cross-sectional scanning electron microscopic (SEM) images on the surfaces of representative multi-scale textured solar cells with black Si etch times of 1.5 and 3 min, respectively. The cross section is prepared by focused ion beam (FIB) with *in-situ* e-beam assisted Pt deposition to enable precise measurement of the nanoporous layer thickness. At micron-scale, neither the shape nor size of the pyramids is significantly altered by the nanoporous Si etch. Even though the pyramid facets are [111] oriented, the nanoscale pores form along the [001] crystal axis, as when we black etch a planar (100) Si surface.⁶

Fig. 2 compares the porous layer depths for as-etched (d_E) and processed solar cell samples (d_{SC}). The etch depths scale linearly with etch time; longer black-etch time gives deeper as-etched pores. However, during subsequent solar

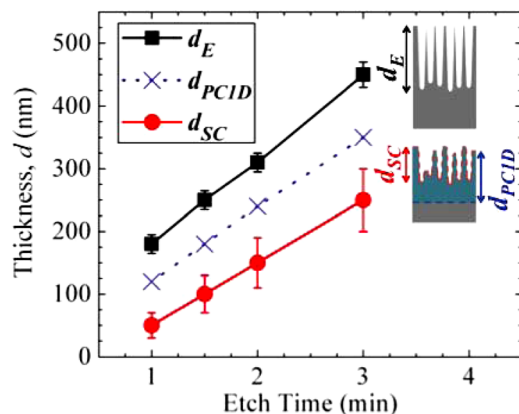


FIG. 2. (Color online) Nanoporous layer thickness as a function of nanoporous black etch time for as-etched, d_E , (square), processed solar cell, d_{SC} , (circle), and electrically “dead layer” thickness as predicted by PC1D solar cell simulation software, d_{PCID} , (cross). The inset shows a schematic depiction of the effect of solar cell processing on the nanoporous layer.

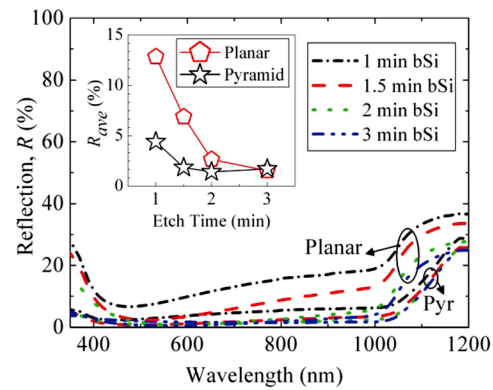


FIG. 3. (Color online) Reflection spectra of multi-scale textured and planar black Si (bSi) with different metal-assisted nanostructured black etch times. The inset is the spectrum-weighted average reflection (R_{ave}) between 350- and 1000-nm for different etch times.

cell processing steps, the depth of the nanostructured porous layer Si is reduced by about one-third. This decrease in the nanoporous layer depth is mainly due to the consumption of Si during thermal oxidation. The remaining height of Si nanostructures may also vary from pore to pore due to both the etching and oxidation, resulting in variations of pore width and depth (d_{SC}), as depicted schematically in the inset of Fig. 2. Bigger error bars for d_{SC} in Fig. 2 represent the depth variation.

We measure the percent reflection (R) as a function of wavelength (λ) of the multi-scale textured and planar black Si samples. Measurements are taken after the emitter formation and passivation step using a spectrophotometer (Varian, Cary 6000i) with an integrating sphere. Fig. 3 presents $R(\lambda)$ spectra for pyramid and planar nanoporous samples etched for different times. The inset of Fig. 3 shows the solar-spectrum-weighted average reflection, R_{ave} , from 350 to 1000 nm. To reach R_{ave} below 2% requires 3-min of metal-assisted etch time on planar Si ($d_{SC} \sim 250$ -nm). In contrast, in multi-scale textured Si, R_{ave} of 1.8% and 1.4%, requires only 1.5-min ($d_{SC} \sim 100$ -nm) and 2-min ($d_{SC} \sim 150$ -nm) of metal-assisted etching, respectively. Therefore, multi-scale textured Si retains low reflectivity even when the nanoporous layer depth is substantially smaller than on the planar surface.

Fig. 4 presents internal quantum efficiency (IQE, electrons collected per photon absorbed) of the multi-scale

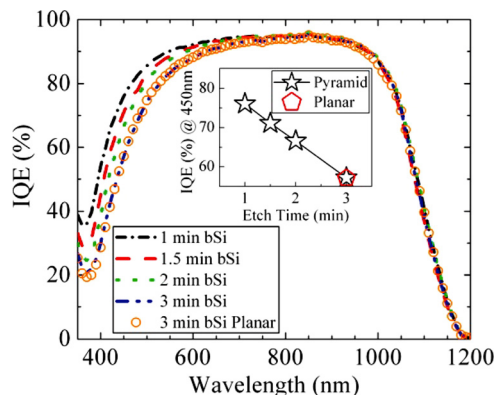


FIG. 4. (Color online) IQE spectrum of multi-scale textured black Si solar cells for different black etch times compared to a 3 min black etched planar solar cell. Inset shows IQE at 450 nm as a function of black etch time.

textured black Si solar cells as well as the planar black Si control; the Fig. 4 inset plots the IQE at 450-nm versus black etch time. The nearly identical IQE of 3-min black-etched cells, whether incorporating multi-scale texture or not, illustrates that the nanoporous layer itself is the performance-limiting factor instead of the ~ 1.3 -times area increase of surface area associated with the pyramids alone. The IQE spectra show that the blue response improves linearly as the black etch time and nanoporous layer depth decrease indicating that nanostructures are far more important for recombination than are the micron-scale structures. Recombination within the nanoporous layer evidently limits the blue IQE. Reference 5 showed that the best fits by PC1D simulation to the black Si IQE data are obtained by representing the nanostructured zone as an electrically “dead layer” of thickness, d_{PC1D} . We PC1D-simulate our cells in this way, with results summarized in Fig. 2. The “dead layer” thickness, d_{PC1D} , is thicker than d_{SC} but thinner than d_E . Two factors may contribute to the nanoporous layer acting as a recombination-active layer with no photovoltaic response in our cells: (1) surface recombination due to the high surface area of the nanoporous layer; and (2) Auger recombination due to heavy emitter doping which is caused by heavy in-diffusion of phosphorus from the high nanostructured surface area. Shallower nanopores reduce both the surface and Auger recombination problems to dramatically improve the blue response in thinner black Si layers.

The NREL Measurements Group independently measured our best multi-scale textured solar cell (1.5-min black etch) to have conversion efficiency of 17.1% with $V_{oc} = 615$ mV, $J_{sc} = 35.6$ mA/cm², and fill factor (FF) of 78.2%, at AM1.5. The diode ideality factor (n) is 1.01 and dark saturation current density (J_0) is 1.87 pA/cm². We note that our record cell has neither the lowest R_{ave} nor the best blue response among the multi-scale textured nanoporous black Si cells we have made. However, this cell has an optimized tradeoff between the IQE and reflectivity. The 1-min black etched cell has the best blue response but it has a lower external QE (EQE) response between 600 and 1000 nm due to a high R_{ave} of 4.2%. The 2-min black etched cell has a lower R_{ave} of 1.4% that leads to a high EQE response from 600 to 1000 nm, but suffers from worse blue response that limits J_{sc} . Compared to the previous best black Si cell on a planar surface, the 1.5-min black etch multi-scale textured cell has about 1.5 mA/cm² higher J_{sc} .

Our experiments clearly show the advantage of multi-scale texturing: it enables the high blue response associated with a very thin nanoporous black Si layer, without sacrificing the excellent AR needed for high black Si solar cell efficiency. A multi-scale texture solar cell with only a 100-nm thick nanostructured layer has similar R_{ave} to a planar cell

with 250-nm nanostructured layer, but the thinner nanostructuring provides better blue response.

In conclusion, we have fabricated a 17.1%-efficient multi-scale textured solar cell without any vacuum-deposited dielectric AR coating. Instead, the AR is achieved by combining the geometric optics advantage of micron scale pyramid texture with a density graded nanoporous black Si layer. We achieve R_{ave} of 1.8% with a nanoporous layer only 100-nm thick on this multi-scale textured cell. Blue response is improved to 71% from 57% by reducing the nanopore depth and, therefore, front-surface recombination. Our results suggest that most high efficiency nanostructured solar cells will be limited in efficiency by recombination of photoexcitation on their high surface areas and will, therefore, benefit from incorporation of light-management strategies that minimize the nanostructured surface area without eliminating the benefits.

This work was supported by the U.S. Department of Energy (DOE) under Contract No. DE-AC36-08-GO28308, through a DOE American Recovery and Reinvestment Act (ARRA) Photovoltaic Supply Chain and Crosscutting Technologies grant. We thank Vern Yost, Anna Duda, Scott Ward, Falah Hasoon, and Jihun Oh for helpful discussions and Paul Ciszek and Keith Emery for cell I-V measurements.

- ¹Q.-B. Vu, D. A. Stricker, and P. M. Zavracky, *J. Electrochem. Soc.* **143**, 1372 (1996).
- ²E. Vazsonyi, K. De Clercq, R. Einhaus, E. V. Kerschaver, K. Said, J. Poortmans, J. Szlufcik, and J. Nijs, *Sol. Energy. Mater. Sol. Cells* **57**, 179 (1999).
- ³P. Panek, M. Lipinski, and J. Dutkiewicz, *J. Mater. Sci.* **40**, 1459 (2005).
- ⁴G. Korotcenkov and B. K. Cho, *Crit. Rev. Solid State Mater. Sci.* **35**, 153 (2010).
- ⁵H.-C. Yuan, V. E. Yost, M. R. Page, P. Stradins, D. L. Meier, and H. M. Branz, *Appl. Phys. Lett.* **95**, 123501 (2009).
- ⁶H. M. Branz, V. E. Yost, S. Ward, K. M. Jones, B. To, and P. Stradins, *Appl. Phys. Lett.* **94**, 231121 (2009).
- ⁷C. H. Crouch, J. E. Carey, J. M. Warrender, J. M. Aziz, E. Mazur, and F. Y. Genin, *Appl. Phys. Lett.* **84**, 1850 (2004).
- ⁸X. Li and P. W. Bohn, *Appl. Phys. Lett.* **77**, 2572 (2000).
- ⁹D. R. Turner, *J. Electrochem. Soc.* **105**, 402 (1958).
- ¹⁰A. Parretta, A. Sarno, P. Tortora, H. Yakuba, P. Maddalena, J. H. Zhao, and A. H. Wang, *Opt. Commun.* **172**, 139 (1999).
- ¹¹H. Sai, H. Fujii, K. Arafune, Y. Ohshita, Y. Kanamori, H. Yugami, and M. Yamaguchi, *Jpn. J. Appl. Phys. Part 1* **46**, 3333 (2007).
- ¹²B. S. Kim, D. H. Lee, S. H. Kim, G. H. An, K. J. Lee, N. V. Myung, and Y. H. Choa, *J. Am. Ceram. Soc.* **92**, 2415 (2009).
- ¹³Y. H. Xiu, S. Zhang, V. Yelundur, A. Rohatgi, D. W. Hess, and C. P. Wong, *Langmuir* **24**, 10421 (2008).
- ¹⁴J. S. Yoo, I. O. Parm, U. Gangopadhyay, K. Kim, S. K. Dhungel, D. Mangalaraj, and S. J. Yi, *Sol. Energy Mater. Sol. Cells* **90**, 3085 (2006).
- ¹⁵M. D. Kelzenberg, S. W. Boettcher, J. A. Petykiewicz, D. B. Turner-Evans, M. C. Putnam, E. L. Warren, J. M. Spurgeon, R. M. Briggs, N. S. Lewis, and H. A. Water, *Nature Mater.* **9**, 239 (2010).
- ¹⁶K. S. Nalwa, J.-M. Park, K.-M. Ho, and S. Chaudhry, *Adv. Mat.* **23**, 112 (2011).
- ¹⁷J. D. Hylton, R. Kinderman, A. R. Burgers, W. C. Sinke, and P. M. M. C. Bressers, *Prog. Photovoltaics* **4**, 435 (1996).